International Journal of Heat and Mass Transfer 81 (2015) 272–282

Contents lists available at ScienceDirect

International Journal of Heat and Mass Transfer

journal homepage: www.elsevier.com/locate/ijhmt

On the determination of parameters required for numerical studies of heat and mass transfer through textiles – Methodologies and experimental procedures

S.F. Neves [a,b], J.B.L.M. Campos [b], T.S. Mayor [c,*]

[a] Nanolayer Coating Technologies, LDA, Rua Fernando Mesquita, 2785, 4760-034 Vila Nova de Famalicão, Portugal
[b] Centro de Estudos de Fenómenos de Transporte (CEFT), Departamento de Engenharia Química, Faculdade de Engenharia da Universidade do Porto, Rua Roberto Frias, 4200-465 Porto, Portugal
[c] Swiss Federal Laboratories for Materials Science and Technology (EMPA), Lerchenfeldstrasse 5, 9014 St. Gallen, Switzerland

ARTICLE INFO

Article history:
Received 9 April 2014
Received in revised form 22 August 2014
Accepted 18 September 2014
Available online 4 November 2014

Keywords:
Textile characterisation
Evaporative resistance
Heat and mass transfer simulation
Convective coefficients
Water sorption
Tortuosity

ABSTRACT

The aim of this study was to develop methodologies and experimental procedures to determine textile parameters required in numerical approaches of heat and mass transfer through textiles. Privileging techniques usually available in textile/clothing laboratories, experimental approaches were defined that allow to estimate all required parameters, while taking into consideration water presence in the fibres and hence the effect of fibres hygroscopic properties. Numerical models usually require values of textile thickness, fibre fraction, and tortuosity, as well as knowledge of the boundary conditions, e.g. convective heat and mass transfer coefficients. To calculate these parameters, thickness, weight, and volume of textile samples were measured, whereas convective and textile evaporative resistances were determined by indirect measurements. Results were obtained for four distinct textile samples (made of wool, cotton, and a mixture of materials), of different hydrophilic nature. When the obtained parameters were incorporated in a numerical model and numerical predictions of temperature and humidity were compared with experimental data obtained during measurements of fabric evaporative resistance, it was shown that the predictions were accurate; this lends support to the developed methods and approaches.

Since an uncertainty in the measured parameters can compromise the accuracy of numerical predictions, a sensitivity analysis was conducted to study the influence of deviations in the model input parameters and of assumptions regarding water presence in the fibres, on the predictions of heat and mass transfer rates. The results show that a deviation in textile weight and thickness as well as the assumption of no water retained in fibres during their characterisation, have a significant effect on the predicted heat transfer and water distribution over time. Moreover, a deviation in the total evaporative resistance, convective evaporative resistance, and sorption rate factor has great influence on the heat flux obtained in the initial period of testing.

1. Introduction

In many different activities, clothing is expected to offer humans the possibility to work comfortably in challenging environments. From fire-fighters to cold chamber operators, from furnace technicians to winter sports athletes, all rely on clothing protective capacity to perform while exposing their bodies to minimal thermal burden. This requires the capacity to optimise and fine-tune clothing properties based on frequently opposing requirements, i.e. protection and thermal comfort. This, together with an increasing need to shorten development cycles, is steering clothing manufactures and developers towards the use of numerical approaches as a way to fine-tune performance according to a set of goals.

Several works in literature report studies on the heat and mass transport in textile structures [1–9]. Le et al. [1] and Gibson and Charmchi [9] used volume-averaging techniques to address the interaction between heat and mass transfer, and track concentration and temperature fronts as moisture is transported through hygroscopic materials. Barker et al. [3] used a similar approach to analyse the role of moisture transport in the protection offered by firefighter garments exposed to high intensity thermal radiation. Fan and co-workers [5–7] studied the heat and mass

* Corresponding author. Tel.: +41 58 7657020; fax: +41 58 7656962.
E-mail addresses: tiago.sottomayor@empa.ch, tiagosmayor@gmail.com (T.S. Mayor).

http://dx.doi.org/10.1016/j.ijheatmasstransfer.2014.09.038
0017-9310/

Nomenclature

A	area [m^2]
C	concentration [$kg\ m^{-3}$]
C_p	specific heat [$J\ kg^{-1}\ K^{-1}$]
d	fibre diameter [m]
D_a	diffusivity of water vapour in air [$m^2\ s^{-1}$]
D_{ef}	effective diffusivity of gas [$m^2\ s^{-1}$]
D_f	diffusivity of water in fibre [$m^2\ s^{-1}$]
h_c	convective heat transfer coefficient [$W\ m^{-2}\ K^{-1}$]
h_m	convective mass transfer coefficient [$m\ s^{-1}$]
k	thermal conductivity [$W\ m^{-1}\ K^{-1}$]
L	thickness [m]
Le	Lewis number [–]
$\dot{m}_{sv}$	mass rate desorption of water from fibre to the gaseous phase [$kg\ s^{-1}\ m^{-3}$]
M_{H_2O}	molar mass of water [$kg\ mol^{-1}$]
p	partial pressure [Pa]
$\dot{q}$	heat flux [$W\ m^{-2}$]
Q_l	enthalpy of water desorption from fibre to the liquid phase [$J\ kg^{-1}$]
r	fibre radius [m]
R	gas constant [$J\ K^{-1}\ mol^{-1}$]
$Regain_{eq}$	equilibrium regain $\left[kg_{H_2O}\ kg_{fibre}^{-1}\right]$
$Regain_{f(\varphi=65)}$	equilibrium regain for φ = 65% $\left[kg_{H_2O}\ kg_{fibre}^{-1}\right]$
$Regain_t$	instantaneous regain $\left[kg_{H_2O}\ kg_{fibre}^{-1}\right]$
$Ret_{textile}$	textile evaporative resistance [$s\ m^{-1}$]
Ret_{total}	total evaporative resistance [$s\ m^{-1}$]
Ret_0	convective evaporative resistance [$s\ m^{-1}$]
$Ret_{textile}^{ISO}$	textile evaporative resistance obtained according to standard [$m^2\ Pa\ W^{-1}$]
Ret_{total}^{ISO}	total evaporative resistance obtained according to standard [$m^2\ Pa\ W^{-1}$]
Ret_0^{ISO}	convective evaporative resistance obtained according to standard [$m^2\ Pa\ W^{-1}$]
T	temperature [K]

Greek letters

Δh_{vap}	water vaporisation enthalpy [$J\ kg^{-1}$]
ε	volume fraction [–]
ρ	density [$kg\ m^{-3}$]
τ	tortuosity [–]
φ	relative humidity [–]

Subscripts

a	air
amb	ambient
bw	bounded water
ds	dry fibre
ef	effective
f	fibre
sat	saturation
v	water vapour
0	initial condition
γ	gas phase
σ	solid phase

transfer across several textile assemblies. They considered different assumptions regarding the mechanisms for water transport, in order to analyse the effect of textile properties and of layers relative position, on the heat and mass transferred across clothing.

The use of numerical approaches to address the study/optimisation of clothing performance requires knowledge of parameters characterising the properties of the textiles (e.g. porosity and tortuosity) and the transport rates of heat and mass across their structure (e.g. diffusion and convective coefficients). However, the measurement of some of these parameters is not straightforward and requires access to complex/expensive experimental facilities [1,9]. Furthermore, in some of the available literature [1–9], it is not entirely clear how some parameters are determined (e.g. porosity, tortuosity) which renders difficult the comparison of results from different authors and may hamper a faster adoption of numerical approaches in clothing development activities.

The transport rates across a textile material depend on several parameters, e.g. thickness of the material, porosity and tortuosity of the fibre structure, and fibre affinity with water. Two textiles made of the same type of fibres but with different porosities may have very different thermal performances. Porosity of a textile is usually determined by evaluating fibre and textile densities, the latter being often determined by weighing a specific volume of textile [10,11,13–16]. However, depending on the hydrophilic nature of the fibre, it retains more or less water. For instance, if polyester is exposed to a humidity of 50%, the equilibrium water content in the fibre (i.e. its regain) corresponds to 1% of the total mass of dry fibre [17]. Yet, in the same conditions, wool fibres reaches equilibrium with a water content corresponding to 11% of its total dry mass [17]. Thus, fibre affinity with water influences textile porosity. This means that the usual methods to determine porosity, which neglect the present of water [10,11], imply a certain degree of uncertainty. Given the influence of this parameter on the heat and mass transport rates across textiles, it results that a new method to determine textile porosity considering the water retained in fibres is needed.

From a transfer point of view, an increase in water retention in the fibres implies a decrease in the gas fraction and, thus, a decrease in the thermal resistance [18]. Furthermore, since the transport of water through the porous network of a textile is dependent on its complexity, an increasing sinuousness or tortuosity implies slower transport. Expressions relating textile tortuosity and porosity are reported in the literature [11,12], however, they refer to specific textiles and were developed neglecting the presence of water accumulated in the fibres. Given the mentioned effect of water retention on textile structure (and hence on its transport properties), there is a clear need for a new method to determine textile tortuosity taking into account the water retained in fibres. This is particularly important to improve the accuracy of the characterisation efforts that precede numerical approaches on the heat and mass transport across textiles.

Against this background, methodologies and experimental procedures were developed to determine the parameters required to study numerically the heat and mass transfer in textiles, while considering the presence of water retained in the fibres. Preference was given to techniques based on equipment usually available in textile/clothing laboratories to contribute to a wider adoption of similar approaches in textile/clothing development activities. The parameters usually required for numerical studies on the heat and mass transport in textiles (i.e. fibre fraction, tortuosity, and mass/heat transfer coefficients), were determined through measurements of textile thickness, weight and volume, as well as of convective and evaporative resistances. Based on the obtained parameters, a model of the heat and mass transfer through textile

materials was developed, which was validated against experimental data of humidity and temperature histories obtained during evaporative resistance tests. The developed model was then used to conduct a sensitivity analysis on the influence of the experimentally-determined parameters, and of assumptions regarding water presence in the fibres, on the numerical predictions of the heat and mass transport rates through textiles.

2. Formulation of the transfer model

A textile can be modelled as a porous material made of fibres, bounded water in fibres, and gas (air and water vapour). In terms of volume faction, the following holds,

$$\varepsilon_{ds} + \varepsilon_{bw} + \varepsilon_{\gamma} = 1 \tag{2.1}$$

where ε_{ds} is the volume fraction of fibres, ε_{bw} the volume fraction of bounded water in fibres, and ε_{γ} the volume fraction of gas.

Following the formulation described by Gibson and Charmchi [9], the textile can be seen as a homogeneous medium with two phases: a gaseous phase (air and water vapour) and a solid phase (fibre and bounded water in fibres). Furthermore, the bounded water in fibres can be assumed immobile and in equilibrium with the water vapour in the pores, and the gas phase behaviour can be assumed ideal.

Considering the above assumptions [9] and a one-dimensional approach to the heat transfer along textile thickness, one can express the conservative energy equation for the textile control volume by,

$$\rho_{ef} \cdot C_{p_{ef}} \cdot \frac{\partial T}{\partial t} + \frac{\partial}{\partial x}\left(-k_{ef} \cdot \frac{\partial T}{\partial x}\right) + \dot{m}_{sv} \cdot (\Delta h_{vap} + Q_1) = 0 \tag{2.2}$$

where the first term represents the accumulation of energy in the textile control volume, the second the heat transferred by conduction, and the third the energy associated with the sorption/desorption of water between the fibres and the gaseous phase. The textile effective properties of Eq. (2.2) such as density (ρ_{ef}), specific heat (Cp_{ef}), and thermal conductivity (k_{ef}; [19]) can be expressed by Eqs. (2.3)–(2.5) (see nomenclature section for details).

$$\rho_{ef} = \varepsilon_{bw} \cdot \rho_w + \varepsilon_{\gamma} \cdot \rho_{\gamma} + \varepsilon_{ds} \cdot \rho_{ds} \tag{2.3}$$

$$Cp_{ef} = \frac{\varepsilon_{bw} \cdot \rho_w \cdot Cp_w + \varepsilon_{\gamma} \cdot (Cp_a \cdot \rho_a + Cp_v \cdot \rho_v) + \varepsilon_{ds} \cdot \rho_{ds} \cdot Cp_{ds}}{\rho_{ef}} \tag{2.4}$$

$$k_{ef} = k_{\gamma} \cdot \left\{\frac{\varepsilon_{\gamma} \cdot k_{\gamma} + [1 + \varepsilon_{bw} + \varepsilon_{ds}] \cdot k_{\sigma}}{\varepsilon_{\gamma} \cdot k_{\sigma} + [1 + \varepsilon_{bw} + \varepsilon_{ds}] \cdot k_{\gamma}}\right\} \tag{2.5}$$

The thermal conductivity of the solid phase (k_{σ}) can be calculated by,

$$k_{\sigma} = \frac{k_w \cdot \rho_w \cdot \varepsilon_{bw} + k_{ds} \cdot \rho_{ds} \cdot \varepsilon_{ds}}{\rho_w \cdot \varepsilon_{bw} + \rho_{ds} \cdot \varepsilon_{ds}} \tag{2.6}$$

In the previous equations, typical values of density, specific heat, and thermal conductivity of water and fibre (subscripts w and ds, respectively) can be found in literature [9], while the fractions of fibre, bounded water, and gas depend on textile structure and on the type of material. For this reason, a procedure was developed to determine these parameters.

The gas thermal conductivity (k_{γ}), gas specific heat (Cp_{γ}), gas pressure (p_{γ}), air partial pressure (p_a), water vapour partial pressure (p_v), dry air density (ρ_a), and gas density (ρ_{γ}) are described by Eqs. (2.7)–(2.12).

$$k_{\gamma} = \frac{k_v \cdot \rho_v + k_a \cdot \rho_a}{\rho_v + \rho_a} \tag{2.7}$$

$$Cp_{\gamma} = \frac{Cp_a \cdot \rho_a + Cp_v \cdot \rho_v}{\rho_{\gamma}} \tag{2.8}$$

$$p_a = p_{\gamma} - p_v \tag{2.9}$$

$$p_v = \frac{\rho_v \cdot R \cdot T}{M_{H_2O}} \tag{2.10}$$

$$\rho_a = \frac{p_a \cdot M_{ar}}{R \cdot T} \tag{2.11}$$

$$\rho_{\gamma} = \rho_a + \rho_v \tag{2.12}$$

The enthalpy of water desorption from the fibre (Q_1; [17]) and the enthalpy of water vaporisation (Δh_{vap}; [9]) are described by Eqs. (2.13)–(2.16), respectively (see nomenclature section for details).

$$Q_1 = 1.95 \times 10^5 \cdot (1 - \varphi) \cdot \left[(0.2 + \varphi)^{-1} + (1.05 - \varphi)^{-1}\right] \tag{2.13}$$

$$\varphi = \frac{p_v}{p_{sat}} \tag{2.14}$$

$$p_{sat} = 614.3 \cdot \exp\left(17.06 \cdot \left[\frac{T - 273.15}{T - 40.25}\right]\right) \tag{2.15}$$

$$\Delta h_{vap} = 2.792 \times 10^6 - 160 \cdot T - 3.43 \cdot T^2 \tag{2.16}$$

The mass desorption rate of water from fibre to the gaseous phase ($\dot{m}_{sv}$) is given by Eq. (2.17) (see Appendix A), as a function of the instantaneous and equilibrium regain of the fibre, $Regain_t$ and $Regain_{eq}$ respectively. These are the instantaneous and equilibrium values of the ratio between the mass of water retained in the fibre and the mass of dry fibre [20]. These ratios can be obtained by Eqs. (2.18) and (2.19) [17],

$$\dot{m}_{sv} = \frac{16 \cdot D_f \cdot \varepsilon_{ds} \cdot \rho_{ds}}{d_f^2} \cdot [Regain_t - Regain_{eq}] \tag{2.17}$$

$$Regain_t = \frac{\varepsilon_{bw} \cdot \rho_w}{\varepsilon_{ds} \cdot \rho_{ds}} \tag{2.18}$$

$$Regain_{eq} = \frac{\varepsilon_{bw}|_{eq} \cdot \rho_w}{\varepsilon_{ds} \cdot \rho_{ds}} = 0.578 \cdot Regain_{f(\varphi=65\%)} \cdot \varphi \cdot \left[(0.321 + \varphi)^{-1} + (1.262 - \varphi)^{-1}\right] \tag{2.19}$$

whereas the ratio between the diffusivity of water in the fibre (D_f) and the square diameter of fibre (d_f^2) is a sorption rate factor which considers the actual fibre/yarn shape and size distribution. This ratio is usually chosen to fit the experimental data [21].

The continuity equation in the textile is expressed as,

$$\frac{\partial(\varepsilon_{\gamma} \cdot \rho_v)}{\partial t} + \frac{\partial}{\partial x}\left(-D_{ef} \cdot \frac{\partial \rho_v}{\partial x}\right) - \dot{m}_{sv} = 0 \tag{2.20}$$

where the first term of the equation represents the water vapour accumulation in the pores, the second the vapour diffusion through the textile, and the third the mass desorption rate of water from the fibre to the gaseous phase. The effective diffusivity of gas (D_{ef}) is proportional to the fibre fraction and to the diffusivity of water in air (D_a; [17,22]) and is inversely proportional to the textile tortuosity (τ).

$$D_{ef} = \frac{\varepsilon_{\gamma} \cdot D_a}{\tau} \tag{2.21}$$

$$D_a = 2.23 \times 10^{-5} \cdot \left(\frac{T}{273.15}\right)^{1.75} \tag{2.22}$$

The tortuosity parameter is specific of each textile, thus, a methodology was developed to determine it.

The continuity equation of water retained in fibre is described by Eq. (2.23).

$$\rho_w \frac{\partial \varepsilon_{bw}}{\partial t} + \dot{m}_{sv} = 0 \tag{2.23}$$

To solve the above set of equations describing the coupled heat and mass transfer through a textile, one needs to determine several parameters such as textile thickness, fraction of fibre, tortuosity, as well as parameters required to obtain heat and mass transfer rates, i.e. the sorption rate factor, and the convective heat and mass transfer coefficients. For this reason, methodologies and experimental procedures were developed to obtain these parameters, while taking into consideration the presence of water in the fibres. This is particularly important because the water retained in fibres, which depends on their affinity with water, influences the characteristics of the textile structure (e.g. porosity and tortuosity) and, hence, the transport rates observed across textiles.

3. Experimental approaches and results

This section describes the procedures that were developed to determine the parameters needed for the modelling/simulation of the heat and mass transfer across textiles (Section 3.1). Section 3.1.1 describes the experimental procedures developed to determine the characteristics and transport rates of four different textile samples. Section 3.1.2 provides details on the data collection for assessing the accuracy of the experimental approaches and validation of the resulting heat and mass transfer model. Finally, the characteristics and transport rates obtained for each of the tested samples are shown in Section 3.2.

3.1. Methodologies and procedures

3.1.1. Textile characteristics and corresponding transport rates

The **textile thickness (*L*)** was measured with an apparatus featuring a pressure-foot which exerts a specific pressure on the textile [10,14,16]. The measurements were conducted according to the standard ISO 9073-2: 1995 [23] and applying a constant pressure of 1.1 kPa to the textile.

The **fraction of fibre (ε_{ds})** in a given textile can be considered constant as long as the textile thickness remains constant and the fibre is assumed not to shrink or swell [21]. The fractions of gas (ε_γ) and retained water in fibre (ε_{bw}) are functions of the ambient conditions to which the textile is exposed.

The usual approaches to determine the fraction of fibre neglect the presence of water retained in textiles [10,11]. Since a deviation in the measured parameters can compromise the accuracy of numerical predictions, a new procedure was developed to calculate the fraction of fibre taking into account the presence of water.

The amount of retained water per mass of dry textile (i.e. the equilibrium regain – $Regain_{eq}$) can be estimated using the isotherm of water sorption in the fibre [20],

$$Regain_{eq} = 0.578 \cdot Regain_{f(\varphi=65\%)} \cdot \varphi \cdot \left[(0.321 + \varphi)^{-1} + (1.262 - \varphi)^{-1}\right] \tag{3.1}$$

where $Regain_{eq}$ is function of the relative humidity in the pores (φ) and of the standard equilibrium regain for φ = 65% ($Regain_{f(\varphi=65)}$; [17]), as estimated from literature (see Appendix B). The equilibrium regain ($Regain_{eq}$) can be related with the fraction of retained water (ε_{bw}) and the fraction of fibre (ε_{ds}) by,

$$\varepsilon_{ds} = \frac{\varepsilon_{bw} \cdot \rho_w}{\rho_{ds} \cdot Regain_{eq}} \tag{3.2}$$

where the density of water (ρ_w) and the density of the fibre (ρ_{ds}) can be estimated through values reported in the literature (see Appendix B). In order to close the problem, a further equation is needed to relate the several fractions (ε_{ds}, ε_{bw}, and ε_γ) with the textile effective density (ρ_{ef}),

$$\rho_{ef} = \varepsilon_{bw} \cdot \rho_{bw} + \varepsilon_{ds} \cdot \rho_{ds} + \varepsilon_\gamma \cdot \rho_\gamma \tag{3.3}$$

The textile effective density (ρ_{ef}) was calculated by weighing a known volume of sample [10,11,13–15], after stabilisation of its moisture content (by exposure to air environment at 20 °C and 65% of humidity, for at least 16 h). Finally, the fraction of fibre (ε_{ds}), of retained water (ε_{bw}), and of gas (ε_γ) were obtained by solving Eqs. (2.1), (3.1), (3.2), (3.3).

The **tortuosity (τ)** is, by definition, directly proportional to the textile evaporative resistance ($Ret_{textile}$)

$$Ret_{textile} = \frac{L}{D_{ef}} = \frac{L}{D_a \cdot \varepsilon_\gamma} \cdot \tau \tag{3.4}$$

which can be modified to

$$\tau = Ret_{textile} \cdot \frac{D_a \cdot \varepsilon_\gamma}{L} \tag{3.5}$$

The thickness (L) and the fraction of gas (ε_γ) can be obtained by the procedures described above, and the diffusivity of water vapour in air (D_a) can be determined through Eq. (2.22) [17,22].

The textile evaporative resistance in Eq. (3.5) ($Ret_{textile}$) can be obtained by an indirect measurement using a sweating guarded hotplate, based on the international standard ISO 11092:1993 (E) [24]. Fig. 1 shows the sketch of experimental apparatus, consisting of an adjustable platform (1, Fig. 1a) surrounded by a thermal guard (4, Fig. 1a) and placed within a cavity in a measuring table (5, Fig. 1a).

Before entering the apparatus, the water is preheated to 35 °C. To evaporate the supplied water, an electrical heating element is used (3, Fig. 1a), with an incorporated temperature control system (2, Fig. 1a). Since the plate has pores and is covered by a water-vapour permeable membrane, only gas passes through the plate.

During the test, the sample is placed over the plate platform (1, Fig. 1b), whose position is adjustable so that the sample upper surface is coplanar with the measuring table. The surface of the sample facing the plate is exposed to a saturated current of water vapour, while the other surface is exposed to a constant air flow (1 m s^{-1}) at 35 °C and 40% relative humidity. During the test, the temperature of the plate is monitored and kept constant by automatic adjustments of the heating provided by the equipment. The test ends when all monitored variables reach steady-state. Before and between measurements, the textiles samples are stabilised in temperature and moisture content, in a climatic chamber at 35 °C and 40% humidity.

At steady-state, the transport rate of water vapour through the textile ($\dot{m}$) is proportional to the difference of water vapour concentrations between the plate (C_{plate}) and the ambient (C_{amb}),

$$\dot{m} = \frac{C_{plate} - C_{amb}}{Ret_{total}} \tag{3.6}$$

where Ret_{total} is the total evaporative resistance, i.e. the sum of the textile evaporative resistance ($Ret_{textile}$) and the convective evaporative resistance (Ret_0).

$$Ret_{total} = Ret_{textile} + Ret_0 \tag{3.7}$$

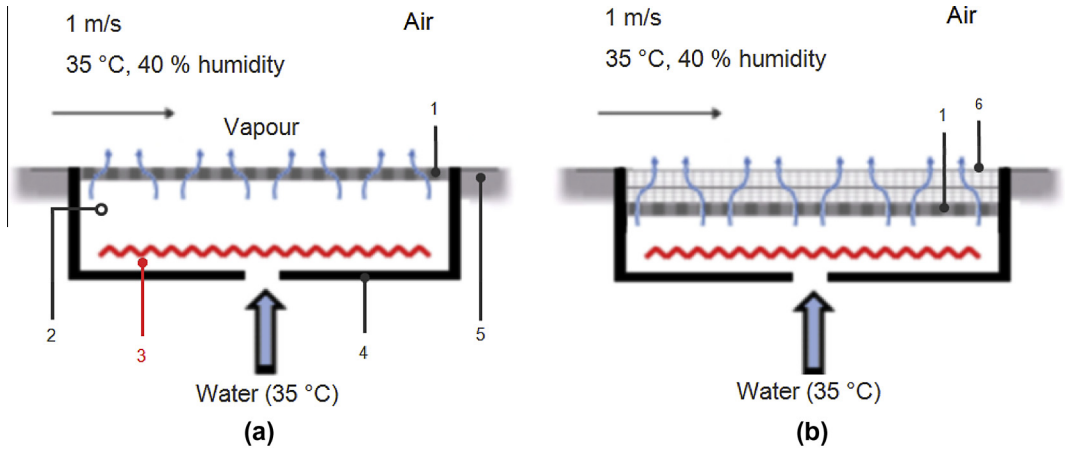

Fig. 1. Experimental set-up to determine the convective (a) and textile (b) evaporative resistances [legend: (1) porous plate with a water-vapour permeable membrane, (2) temperature sensor, (3) heating element, (4) thermal guard, (5) measuring table, and (6) textile sample].

Since the measurements are performed in isothermal conditions (35 °C), the steady-state heat flux required to maintain a constant temperature of the plate($\dot{q}$) is directly proportional to the transport rate of water vapour through the textile ($\dot{m}$), which equals the rate of water evaporation,

$$\dot{q} = \dot{m} \cdot \Delta h_{vap} \tag{3.8}$$

where Δh_{vap} is the water vaporisation enthalpy. Therefore, to determine the total evaporative resistance (Ret_{total}), Eq. (3.8) can be rewritten taking into consideration the ideal gas law and the definition of the water vapour transport rate (Eq. (3.6)), as follows,

$$\dot{q} = \frac{(C_{plate} - C_{amb})}{Ret_{total}} \cdot \Delta h_{vap} = \frac{1}{Ret_{total}} \cdot \Delta h_{vap} \cdot \left[\frac{M_{H_2O}}{R \cdot T} \cdot (p_{v,\ plate} - p_{v,amb})\right] \tag{3.9}$$

which can be modified to

$$Ret_{total} = \Delta h_{vap} \cdot \left[\frac{M_{H_2O}}{R \cdot T}\right] \cdot (p_{v,\ plate} - p_{v,amb}) \cdot \frac{1}{\dot{q}} \tag{3.10}$$

where $p_{v,plate}$ is the partial pressure of water vapour at the surface of the plate (assumed equal to the saturation pressure), $p_{v,amb}$ is the partial pressure of water vapour in the test environment (controlled during the test), T the ambient temperature (35 °C), R the gas constant, and M_{H_2O} the molar mass of water. The total evaporative resistance obtained according to the international standard ISO 11092:1993 (Ret^{ISO}_{total}; [24]), is, by definition,

$$Ret^{ISO}_{total} = \frac{(p_{v,\ plate} - p_{v,amb})}{\dot{q}} \tag{3.11}$$

Thus, by substituting $\dot{q}$ in Eq. (3.10) according to Eq. (3.11), one obtains an expression to calculate the total evaporative resistance (Ret_{total}), based on the values obtained experimentally (Ret^{ISO}_{total}), as follows,

$$Ret_{total} = \Delta h_{vap} \cdot \left[\frac{M_{H_2O}}{R \cdot T}\right] \cdot Ret^{ISO}_{total} \tag{3.12}$$

Finally, to calculate the tortuosity of the textile (Eq. (3.5)) it is necessary to relate the total evaporative resistance (Ret_{total}) with the evaporative resistance of the textile ($Ret_{textile}$). As shown in Eq. (3.7), this requires the definition of the convective (to the ambient) evaporative resistance (Ret_0). To determine Ret_0, the experiment described before was repeated [24] without a sample (Fig. 1a), in order to measure, in the steady-state, the heat flux required ($\dot{q}_0$) to maintain the plate surface at constant temperature. As for the total evaporative resistance (Ret_{total}), the convective evaporative resistance obtained experimentally (Ret^{ISO}_0) was used to determine the convective evaporative resistance (Ret_0) which is used in Eq. (3.7). The tortuosity was then obtained by solving Eq. (3.5).

The methodologies and procedures described before allowed the determination of textile characteristics. However, numerical analyses also require knowledge about the boundary conditions which define the problem, in this case the convective mass and heat transfer coefficients.

The **convective mass transfer coefficient (h_m)** can be calculated as,

$$h_m = \frac{1}{Ret_0} \tag{3.13}$$

where Ret_0 is the convective evaporative resistance [24].

The **convective heat transfer coefficient (h_c)** can be obtained using the *Lewis* equation (Eq. (3.14)), where, for the particular case of mixtures of water vapour in air, the *Lewis* number (Le) takes the value of 1 [25].

$$\frac{h_c}{h_m} = \rho_a \cdot C_{pa} \cdot L_e^{2/3} \tag{3.14}$$

Table 1 summarises the set of approaches and equations used to obtain the characteristics (L, ρ_{ef}, ε_{ds}, and τ) of four distinct samples and also the parameters needed to obtain the corresponding heat and mass transfer rates (h_m, h_c, and D_f/d_f^2).

3.1.2. Data collection for assessment of the experimental approaches' accuracy and validation of the resulting transfer model

The temperature and humidity in the middle of the samples were monitored during the evaporative resistance tests [24] described in the previous section. One temperature/humidity

Table 1
Summary of the approaches and equations used to calculate the parameters required in the numerical simulations.

Parameter	Symbol	Approach	Equations
Thickness	L	[23]	–
Textile effective density	ρ_{ef}	[10,11,13–15]	–
Fibre volume fraction	ε_{ds}	–	(3.1)–(3.3)
Tortuosity	τ	[24]	3.5, 3.7, 3.11
Mass transfer coefficient	h_m	[24]	(3.13)
Heat transfer coefficient	h_c	–	(3.14)
Sorption rate factor	D_f/d_f^2	[21]	–

Table 2
Description and parameters of the four samples analysed (5 independent measurements for L and ρ_{ef}; 3 independent measurements for ε_{ds}, and τ; 95% confidence interval).

Sample	Composition	Description	L [mm]	ρ_{ef} [kg m^{-3}]	ε_{ds} [–]	τ [-]
I	100% wool	–	8.57 ± 0.18	103.6 ± 2.1	0.069 ± 0.001	1.18 ± 0.09
II	100% cotton	–	0.74 ± 0.05	350.6 ± 24.4	0.211 ± 0.015	2.48 ± 0.28
III	100% cotton	Wrinkled surface	3.63 ± 0.15	201.1 ± 8.3	0.130 ± 0.005	1.32 ± 0.08
IV	Layer 1 – 100% cotton Layer 2 – 80% wool 20% polyamide	Sample with 2 different type of layers	6.00 ± 0.09	165.0 ± 2.5	0.116 ± 0.002	1.24 ± 0.07

sensor (with a response time of 5 s and a resolution of 0.1 °C and 0.1% in temperature and humidity, respectively) was placed sandwiched between the two layers of each sample, at the geometrical centre. This allowed collecting temperature and humidity histories during the tests, for direct comparison with the numerical predictions obtained with the implemented transfer model. Details on this comparison are given in Section 4.2.

3.2. Experimental results

The parameters obtained for four different samples are shown in Table 2.

From the four tested samples, three were made of pure fibre (cotton or wool) while the fourth is a mixture of materials. For that reason, the properties of sample IV (ρ_{ef}, ε_{ds}, and τ) were defined based on a weighted average of the properties of the materials in higher proportion (wool and cotton; Table 3). The several textiles parameters shown in Table 2 are in good agreement with the results reported by other authors [1,9,12,26–28].

The experimental convective mass transfer coefficient is 0.01 m s^{-1} and it was obtained assuming a flat textile surface (equivalent to the plate apparatus surface [24]; Fig. 1a). The convective heat transfer coefficient was calculated using Eq. (3.14), based on the obtained experimental convective mass transfer coefficient.

4. Numerical simulation of heat and mass transfer through textiles

The parameters obtained through the experimental procedures described in Section 3.1.1 were used as input to model the heat and mass transfer across the tested samples. After implementation (Section 4.1), the model was used to simulate numerically the conditions of the evaporative tests [24], in order to obtain numerical predictions of temperature and humidity, in the middle of the samples. In Section 4.2, these numerical predictions are directly compared with the experimental data of temperature and humidity collected during the evaporative tests [24], in order to assess the experimental procedures' accuracy and validate the implemented transfer model. In Section 4.3, the model is used to conduct a sensitivity analysis of the influence of several parameters on the heat and mass transport rates across the samples.

4.1. Modelling assumptions, approach and boundary conditions

A finite element approach was used to solve the governing equations expressing energy conservation (Eq. (2.2)), mass transfer in the textile (Eq. (2.20)), and water retention in the fibre (Eq. (2.23)). For the purpose, a second order discretization scheme, a time-step of 0.01 s and a maximum number of mesh elements of 1200 (found adequate to ensure grid-independent results) were used. The 1D model considers a surface exposed to a saturated current of water vapour (surface facing the plate; Fig. 1b) while the other surface is exposed to a constant air flow (1 m s^{-1}), at 35 °C and 40% of relative humidity (surface facing the air flow; Fig. 1b). This implies the use of a Dirichlet boundary condition for heat and mass transfer, at the surface facing the plate (i.e. constant plate temperature and relative humidity, Table 3) and a Newman boundary condition at the surface exposed to the air flow (i.e. convective coefficients). For initial conditions, it was assumed that the textile is uniform in temperature and humidity and it is in equilibrium with the humidity recorded at the beginning of the experiments (Table 3). At each time step, the temperature along the textile is calculated by Eq. (2.2) while the fractions of gas and bounded water are evaluated by Eqs. (2.20) and (2.23), respectively. The mass desorption rate of water from fibre to the gaseous phase is calculated by Eq. (2.17). The properties of the textile samples, water, and air used in the numerical simulations are shown in Table 3.

4.2. Model validation

Fig. 2 shows the evolution over time of the numerical and experimental temperature and humidity at the middle of the sample, for the four textiles samples considered in the study (Table 2).

Both numerical and experimental temperature profiles over time shown in Fig. 2a, c, e, and g exhibit a significant increase of temperature during the first minutes. When the sample is exposed to the saturated current of water vapour, a portion of the vapour condensates and is sorbed by fibres, which results in the release of energy and the corresponding temperature increase. In line with this, the most hygroscopic sample (sample I, Fig. 2a), shows the highest increase of temperature, with a peak temperature of 38.7 °C (i.e. 5 °C above the sample initial temperature).

The comparison of the numerical and experimental temperature profiles shows that the maximum deviation occurs for sample I, in the steady-state (Fig. 2a), where the temperature prediction is 2 °C higher than the experimental value. The numerical and experimental humidity profiles also show interesting agreement and consistent evolution over time (despite bigger deviations at the initial instants of the test, when higher variations of water vapour partial pressure and saturation vapour pressure are expected). These results indicate that the methods and approaches developed to characterise textiles while taking into account the presence of water in their structure, are representative and accurate. These results also show that the model predicts well temperature and humidity changes over time, and so, it can be used to study heat and mass transfer across textiles.

Using the developed model, the influence of a deviation in the measured parameters on the heat and mass transfer rates through textiles was analysed systematically. The main results of this analysis are discussed in the following section.

4.3. Influence of the methodology adopted to obtain textiles parameters and convective coefficients

Numerical analysis allows the study of several problems related with moisture accumulation within apparels, e.g. chilling discomfort in sportswear [5] or the influence of moisture in the thermal performance of fire-fighter's protective garments [3]. This is relevant because it provides information that is critically important for the optimisation of apparel features and structure, which,

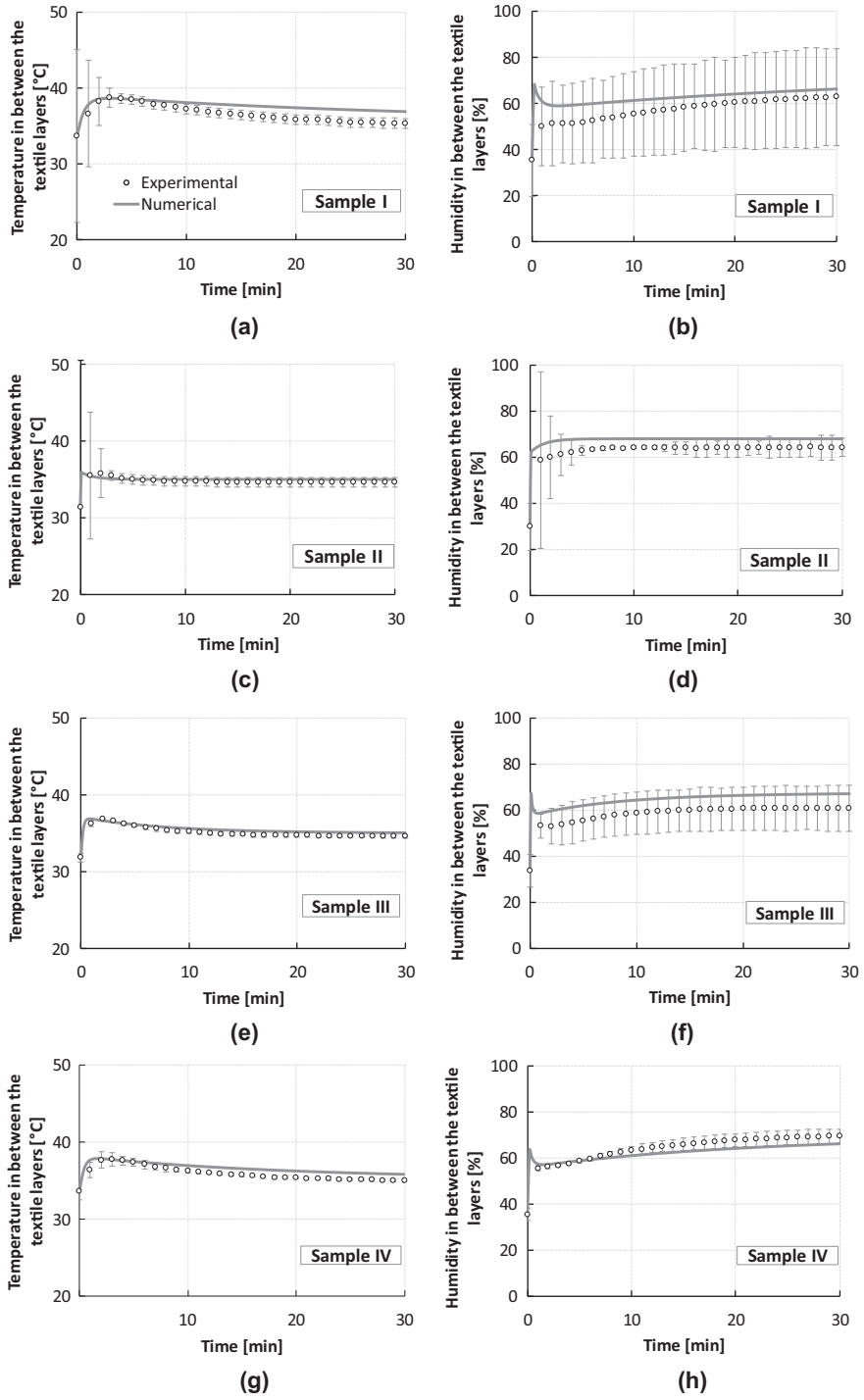

Fig. 2. Experimental and numerical data obtained in between the textile layers of sample I (*a* and *b*), sample II (*c* and *d*), sample III (*e* and *f*), and sample IV (*g* and *h*; Table 2); temperature (*a*, *c*, *e* and *g*) and humidity (*b*, *d*, *f* and *h*) as function of time (2 independent measurements for sample I and II; 3 independent measurements for sample III and IV; 95% confidence interval).

ultimately, determine the user thermal comfort. However, the accuracy of the numerical predictions depends on the precision of textiles parameters used to model the heat and mass transfer phenomena. For that reason, a sensitivity analysis was carried out on the influence of the experimentally-determined parameters, and of assumptions regarding water presence in the fibres, on the numerical predictions of heat and mass transport across textiles. This allowed analysing the consequence of neglecting some of the often-overlooked effects, such as sorption of water vapour in fibres and the resulting change in the structure of the textile porous network. New simulations were done for the most hydrophilic sample (sample I, Table 2), considering the approaches summarised in Table 1, the parameters of Table 3, and a deviation of 20% in the experimental values of several specific parameters. The parameters considered in this study were thickness, weight, total evaporative resistance, convective evaporative resistance, and sorption rate factor. For every analysis, only one parameter was assumed to change (by 20%) relative to what had been

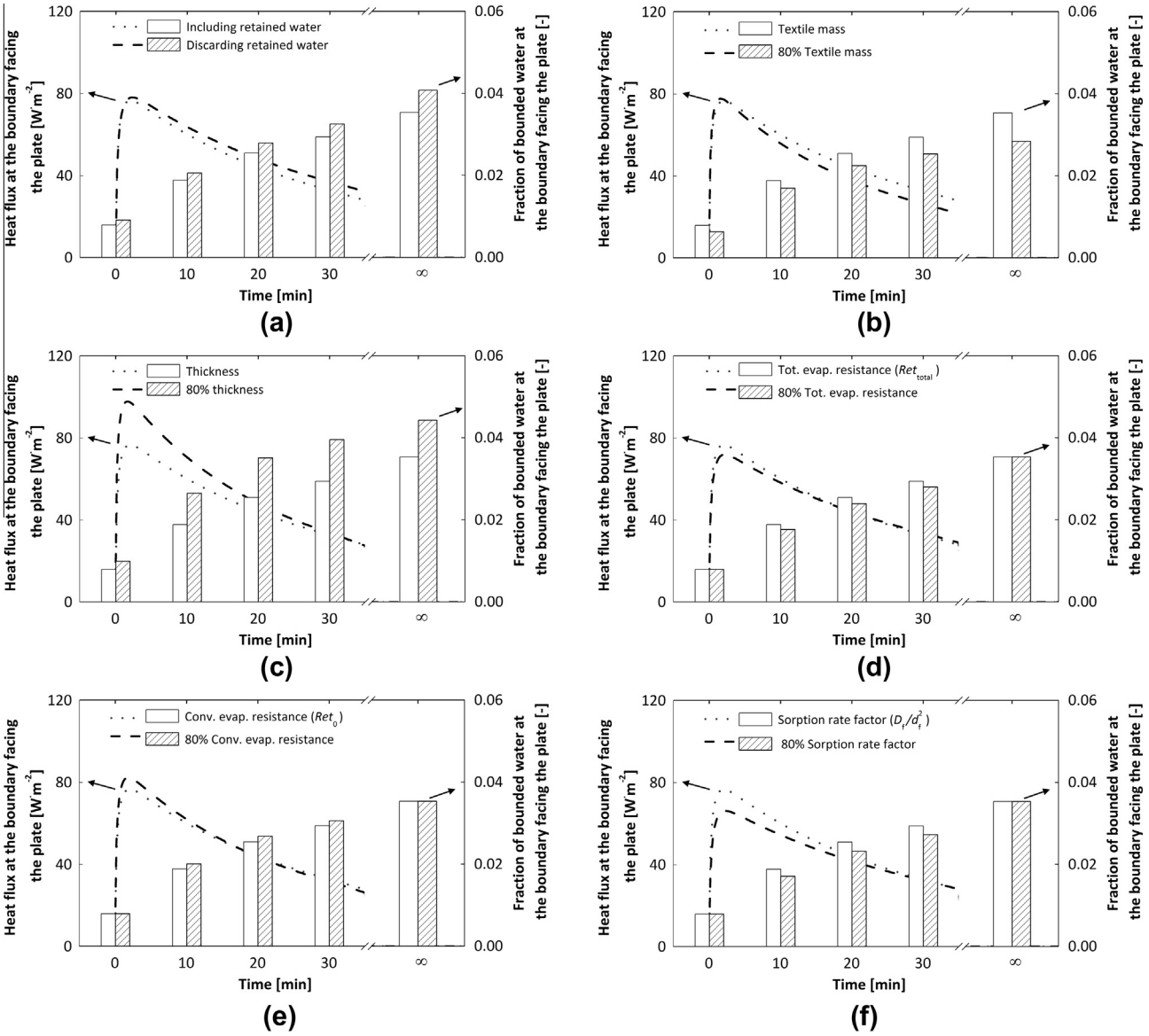

Fig. 3. Numerical prediction of heat flux and fraction of bounded water at the boundary facing the plate, as function of time, for the parameters defined in Table 3, considering deviation as follows: (a) including/discarding retained water in calculation of fibre fraction, (b) with/without underestimation of textile mass; (c) with/without underestimation of textile thickness; (d) with/without underestimation of textile total evaporative resistance; (e) with/without underestimation of convective evaporative resistance; and (f) with/without underestimation of sorption rate factor.

measured, whereas the remaining parameters were assumed to maintain the measured values. Furthermore, it was also assessed the effect of neglecting the water retained in the fibres in the determination of the textile fibre fraction (Fig. 1a).

To enable the interpretation of the results in the context of the effect of apparel on the heat and mass transport from the body, focus was put on the textile boundary facing the plate (Fig. 1b), which can be assumed to represent the skin of a body protected by clothing. Particular attention was given to two parameters that are relevant for the perception of thermal comfort of a clothing user, namely the rate of heat transfer observed at the skin and the amount of water existing near the skin. In Fig. 3, these parameters are represented by the heat flux and fraction of bounded water observed at the textile boundary facing the plate (Fig. 1b).

As shown in Fig. 3a, the assumption regarding the existence/absence of water in the determination of fibre fraction clearly influences the obtained steady-state values. When considering water retention, a fibre fraction of 0.069 is obtained, whereas if water is discarded, a value of 0.079 is obtained. This higher value leads to a lower gas fraction and consequently to a higher textile evaporative resistance. Thus, longer times are needed for heat flux and fraction of bounded water to reach equilibrium resulting, for instances, in a 11% difference in the plate heat flux after 30 min, and a 14% difference in the steady-state values of bounded water fraction (Fig. 3a).

The 20% underestimation of textile mass has also a considerable effect on the results of heat flux and fraction of bounded water over time (Fig. 3b). As shown in Fig. 3b, after 30 min, deviations of 19% and 14% are observed for heat flux and bounded water fraction, respectively. At the steady-state, the fraction of bounded water is underestimated by 20% (Fig. 3b).

Fig. 3c shows that a deviation in the textile thickness has a significant influence in the plate heat flux during the initial period of the experiment. After 2 min, the deviation is about 28%, but after 10 and 30 min the deviation reduces to 17% and 3%, respectively. As shown in Fig. 3c, the fraction of bounded water is overestimated by 25% at the steady-state. The 20% underestimation of the textile thickness leads to a 25% higher value of the textile density and

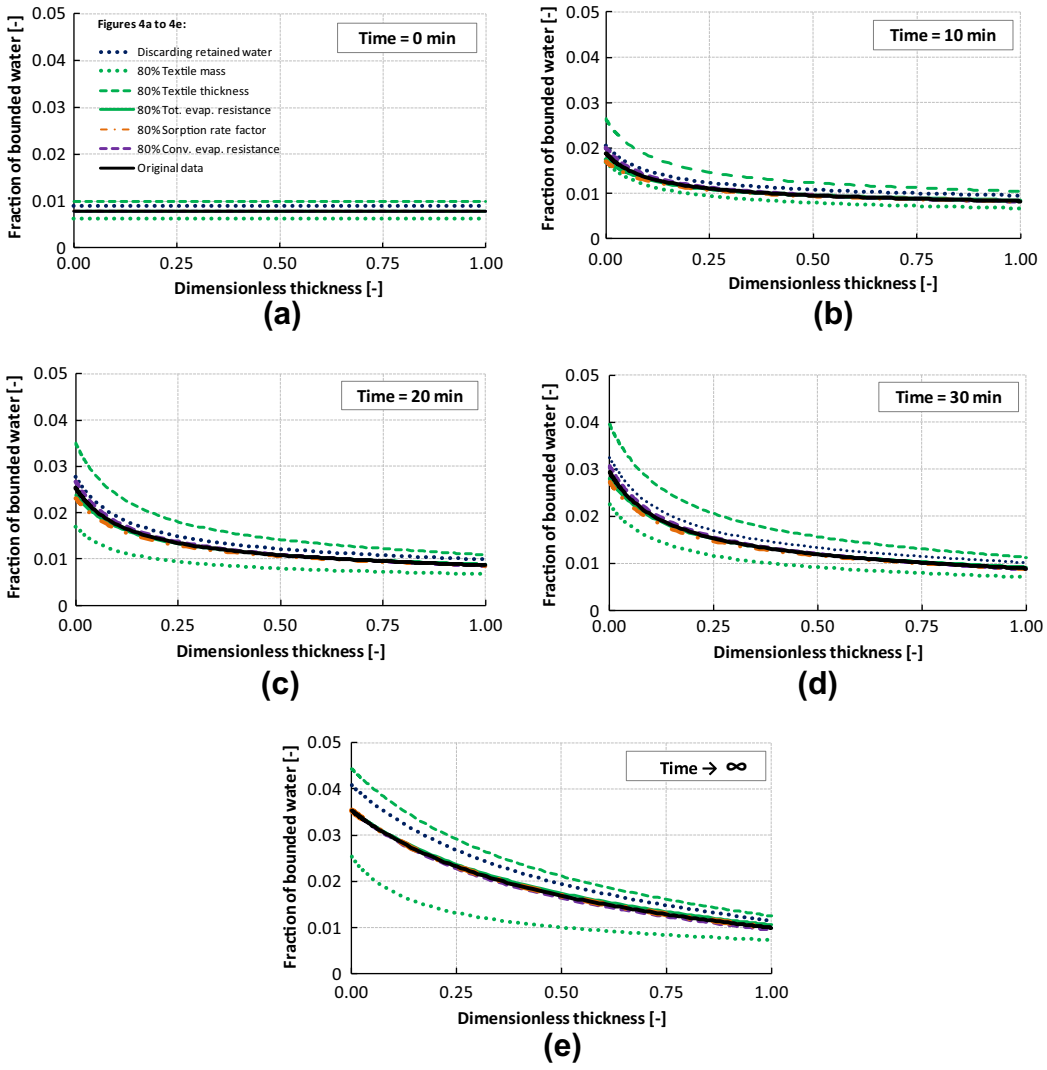

Fig. 4. Fraction of bounded water in fibres along the dimensionless thickness of textile, at different times.

consequently to an overestimation of the fibre fraction by 20% (see Section 3.1).

The deviations in the total evaporative resistance (Fig. 3d), convective evaporative resistance (Fig. 3e), and sorption rate factor (Fig. 3f) have a great influence on the plate heat flux and bounded water fraction at the initial period of the tests. However, the above deviations do not affect the volume fractions of the textile, and for that reason, the fraction of bounded water in the steady-state is the same for all the cases (Fig. 3d, e, and f).

Fig. 4 shows the distribution of bounded water along the dimensionless thickness of the textile, for different times and values of the parameters under analysis.

In Fig. 4, the numerical predictions of bounded water fractions obtained assuming a 20% deviation in the sorption rate factor or in the total and convective evaporative resistances, are very similar and thus, practically overlapped. Significant deviations occur when liquid water retained in fibres is neglected and also when the thickness and the mass of textile are underestimated. As shown in Fig. 4a, at the beginning, if the thickness is underestimated, the fraction of bounded water deviates 25% from the values obtained with the experimental parameters, whereas neglecting the retained water in the calculation of the fibre fraction affects the bounded water fraction by 15%. Over time, the resulting deviation of discarding the retained water in the calculation of fibre fraction diminishes, since the value of the bounded water fraction increases and, consequently, the relative deviation decreases. However, at the steady-state it is still higher than 10% (Fig. 4e). When considering an underestimated mass of textile, the fraction of retained water is underestimated, resulting, at the beginning of the test (Fig. 4a) and at the steady-state (Fig. 4e), in a maximum deviation of 20%. From Fig. 4e, one concludes that, at steady-state, the parameter whose underestimation results in the least accurate predictions is the textile mass.

Either neglecting the retained water in the determination of textile fractions, or underestimating textile thickness, leads to an overestimation of the amount of bounded water. Otherwise, if a lower value of textile mass is used, the water accumulated in the textile is underestimated. A deviation in one of the latter three parameters affects the water distribution along the textile since they are used to determine the fibre fraction (see Section 3.1).

5. Conclusions

Methodologies and experimental procedures were developed to determine parameters required in numerical studies of heat and mass transfer through textiles, using techniques based on equipments usually available in textile/clothing laboratories (e.g.

Table 3
Air, water, samples properties, and initial and boundary conditions defined in numerical simulations.

Sample	Parameter	Unit	Value	Source
I–IV	Cp_v	J kg^{-1} K^{-1}	1862	Ref. [29]
	Cp_w	J kg^{-1} K^{-1}	4190	Ref. [29]
	Cp_a	J kg^{-1} K^{-1}	1003	Ref. [29]
	ρ_w	kg m^{-3}	1000	Ref. [29]
	k_w	W K^{-1} m^{-1}	0.60	Ref. [29]
	k_a	W K^{-1} m^{-1}	2.56×10^{-2}	Ref. [29]
	k_v	W K^{-1} m^{-1}	2.46×10^{-2}	Ref. [29]
	R	J K^{-1} mol^{-1}	8.314	Ref. [29]
	M_{H2O}	kg mol^{-1}	18.02×10^{-3}	Ref. [29]
	M_a	kg mol^{-1}	28.97×10^{-3}	Ref. [29]
	p_{atm}	Pa	101,325	Ref. [29]
	ρ_a (35 °C)	kg m^{-3}	1161×10^{-3}	Ref. [29]
	φ_a	–	0.40	Experimental
	φ_{plate}	–	1.00	Experimental
	T_{plate}	K	308.15	Experimental
I	k_{wool}	W K^{-1} m^{-1}	0.20	Ref. [9]
	Cp_{wool}	J kg^{-1} K^{-1}	1360	Ref. [9]
	ρ_{wool}	kg m^{-3}	1300	Ref. [9]
	$Regain_{f\ -\ wool}$	–	0.15	Ref. [9]
	$D_f/d^2_{f-\ wool}$	s^{-1}	4.88×10^{-4}	Fit
	L_{wool}	m	8.57×10^{-3}	Experimental
	$\varepsilon_{ds\ wool}$	–	0.069	Eqs. (3.1)–(3.3)
	τ_{wool}	–	1.18	Eq. (3.5)
	T_{0wool}	K	306.85	Experimental
	φ_{0wool}	–	0.35	Experimental
II and III	k_{cotton}	W K^{-1} m^{-1}	0.16	Ref. [9]
	Cp_{cotton}	J kg^{-1} K^{-1}	1210	Ref. [9]
	ρ_{cotton}	kg m^{-3}	1550	Ref. [9]
	$Regain_{f\ -\ cotton}$	–	0.07	Ref. [9]
II	$D_f/d^2_{f-\ cotton}$	s^{-1}	1.13×10^{-3}	Fit
	L_{cotton}	m	0.74×10^{-3}	Experimental
	$\varepsilon_{ds\ cotton}$	–	0.215	Eqs. (3.1)–(3.3)
	τ_{cotton}	–	2.46	Eq. (3.5)
	$T_{0cotton}$	K	304.55	Experimental
	$\varphi_{0cotton}$	–	0.30	Experimental
III	$D_f/d^2_{f-\ cotton}$	s^{-1}	2.12×10^{-4}	Fit
	L_{cotton}	m	3.63×10^{-3}	Experimental
	$\varepsilon_{ds\ cotton}$	–	0.130	Eqs. (3.1)–(3.3)
	τ_{cotton}	–	1.32	Eq. (3.5)
	$T_{0cotton}$	K	304.95	Experimental
	$\varphi_{0cotton}$	–	0.34	Experimental
IV	$k_{wool+cotton}$	W K^{-1} m^{-1}	0.18	Weighted average, Ref. [9]
	$Cp_{wool+cotton}$	J kg^{-1} K^{-1}	1285	Weighted average, Ref. [9]
	$\rho_{wool+cotton}$	kg m^{-3}	1425	Weighted average, Ref. [9]
	$Regain_{f\ -\ wool+cotton}$	–	0.11	Weighted average, Ref. [9]
	$D_f/d^2_{f-\ wool+cotton}$	s^{-1}	9.35×10^{-5}	Fit
	$L_{wool+cotton}$	m	6.00×10^{-3}	Experimental
	$\varepsilon_{dswool+cotton}$	–	0.116	Eqs. (3.1)–(3.3)
	$\tau_{wool+cotton}$	–	1.24	Eq. (3.5)
	$T_{0wool+cotton}$	K	306.75	Experimental
	$\varphi_{0wool+cotton}$	–	0.36	Experimental

sweating guarded-hotplate). The developed methodologies and approaches allow to take into account the presence of water in the fibres, and thus, to increase the accuracy of measurements of textile characteristics and corresponding transport properties. Numerical analyses were carried out to assess the accuracy of the developed methods, for four distinct textile samples. The comparison of numerical and experimental data of temperature and humidity, observed in the samples during transient exposures, indicated that the developed methods and approaches are accurate and representative.

A sensitivity analysis was carried out on the influence of several parameters and of assumptions regarding water presence in fibres, on the numerical predictions of heat and mass transport rates observed across textiles. The obtained results show that deviations in textile weight and thickness, as well as the assumption of no water retention in fibres, have a significant effect on the heat transfer and water distribution observed over time. Furthermore, deviations in the total evaporative resistance, convective evaporative resistance, and sorption rate factor have a great influence on the heat transferred through textile, in the initial period of test.

These results stress the importance of considering water presence during textile characterisation activities, as this may impact directly the prediction capacity of heat and mass transfer models. The methodologies and experimental approaches described in this work provide a way to achieve that. This is relevant to allow accurate predictions of apparel thermal performance, which is critically important in optimisation activities (e.g. of protective clothing or sports apparel).

Conflict of interest

None declared.

Acknowledgement

The support provided by Fundação para a Ciência e a Tecnologia (FCT), Portugal under grant number SFRH/BDE/51382/2011 is gratefully acknowledged.

Appendix A

A.1. Mass rate desorption of water from fibre to the gaseous phase, $\dot{m}_{sv}$

The mass desorption rate of water from fibre to the gaseous phase ($\dot{m}_{sv}$) can be obtained by performing a mass balance to the fibre (Eq. (A.1); [1]), assuming that the water is transferred by diffusion along fibre radius, and that the fibre radius is significantly smaller than the fibre length.

$$\frac{1}{r}\frac{d}{dr}\left(r\cdot(-D_f)\frac{dC_f}{dr}\right)+\dot{m}_{sv}=0 \tag{A.1}$$

In Eq. (A.1), r is the fibre radius, D_f the water diffusivity in the fibre, and C_f the water concentration in the fibre. By integrating the above equation taking the following boundary conditions

$$\left.\frac{dC_f}{dr}\right|_{r=0}=0,\quad C_f|_{r=R\text{fibre}}=C_f,\quad \text{and}\quad C_f|_{r=0}=C_{f\,eq},$$

one obtains,

$$\dot{m}_{sv}=\frac{4\cdot D_f}{R_{fibre}^2}\cdot\left(C_f-C_{feq}\right) \tag{A.2}$$

In the above equation, the water concentration (C_f) can be expressed as,

$$C_f=\varepsilon_{bw}\cdot\rho_w \tag{A.3}$$

where ε_{bw} is the fraction of bounded water and ρ_w is the water density. However, considering the definition of fibre regain (Eq. (2.18)), it follows,

$$C_f=\varepsilon_{bw}\cdot\rho_w\Rightarrow C_f=Regain_t\cdot\varepsilon_{ds}\cdot\rho_{ds} \tag{A.4}$$

where ε_{ds} is the fraction of fibre and ρ_{ds} is the fibre density. Thus, Eq. (A.2) can be rewritten as considered in the numerical model (Eq. (2.17)),

$$\dot{m}_{sv}=\frac{16\cdot D_f\cdot\varepsilon_{ds}\cdot\rho_{ds}}{d_f^2}\cdot\left(Regain_t-Regain_{eq}\right) \tag{A.5}$$

Appendix B. Parameters defined in the numerical model

See Table 3.

References

[1] C.V. Le, N.G. Ly, R. Postle, Heat and mass transfer in the condensing flow of steam through an absorbing fibrous medium, Int. J. Heat Mass Transfer 38 (1) (1995) 81–89.
[2] Y. Li, Z. Qingyong, K.W. Yeung, Influence of thickness and porosity on coupled heat and liquid moisture transfer in porous textiles, Text. Res. J. 72 (5) (2002) 435–446.
[3] R.L. Barker, G. Song, H. Hamouda, D.B. Thompson, A.V. Kuznetsov, A.S. Deaton, P. Chitrphiromsri, Modeling of Thermal Protection Outfits for Fire Exposures F01-NS50, 50 (November) North Caroline State, 2004.
[4] J. Fan, X. Cheng, Y.-S. Chen, An experimental investigation of moisture absorption and condensation in fibrous insulations under low temperature, Exp. Therm. Fluid Sci. 27 (6) (2003) 723–729.
[5] H. Wu, J. Fan, Study of heat and moisture transfer within multi-layer clothing assemblies consisting of different types of battings, Int. J. Therm. Sci. 47 (5) (2008) 641–647.
[6] J. Fan, X. Cheng, Heat and moisture transfer with sorption and phase change through clothing assemblies: part II: theoretical modeling, simulation, and comparison with experimental results, Text. Res. J. 75 (3) (2005) 187–196.
[7] J. Fan, X. Cheng, X. Wen, W. Sun, An improved model of heat and moisture transfer with phase change and mobile condensates in fibrous insulation and comparison with experimental results, Int. J. Heat Mass Transfer 47 (10–11) (2004) 2343–2352.
[8] C. Ye, H. Huang, J. Fan, W. Sun, Numerical study of heat and moisture transfer in textile materials by a finite volume method, Commun. Comput. Phys. 4 (4) (2008) 929–948.
[9] P. Gibson, M. Charmchi, The use of volume-averaging techniques to predict temperature transients due to water vapor sorption in hygroscopic porous polymer materials, J. Appl. Polym. Sci. 64 (3) (1997) 493–505.
[10] I. Salopek Čubrić, Z. Skenderi, A. Mihelić-Bogdanić, M. Andrassy, Experimental study of thermal resistance of knitted fabrics, Exp. Therm. Fluid Sci. 38 (2012) 223–228.
[11] C. Brasquet, P. Le Cloirec, Pressure drop through textile fabrics — experimental data modelling using classical models and neural networks, Chem. Eng. Sci. 55 (15) (2000) 2767–2778.
[12] R. Vallabh, Modeling Tortuosity in Fibrous Porous Media Using Computational Fluid Dynamics, Faculty of North Carolina State University, 2009, p. 26.
[13] J.R. Lawson, T.A. Pinder, Estimates of Thermal Conductivity for Materials Used in Fire Fighters' Protective Clothing, Maryland, Gaithersburg, 2000. p. 4.
[14] G. Bedek, F. Salaün, Z. Martinkovska, E. Devaux, D. Dupont, Evaluation of thermal and moisture management properties on knitted fabrics and comparison with a physiological model in warm conditions, Appl. Ergon. 42 (6) (2011) 792–800.
[15] R.M. Laing, S.E. Gore, C.a. Wilson, D.J. Carr, B.E. Niven, Standard test methods adapted to better simulate fabrics in use, Text. Res. J. 80 (12) (2010) 1138–1150.
[16] S. Lee, S.K. Obendorf, Statistical modeling of water vapor transport through woven fabrics, Text. Res. J. 82 (3) (2012) 211–219.
[17] N. Pan, P. Gibson, Thermal and Moisture Transport in Fibrous Materials, first ed., Wookhead Publishing Limited, 2006. pp. 336, 427.
[18] P.W. Gibson, M. Charmchi, Modeling convection/diffusion processes in porous textiles with inclusion of humidity-dependent air permeability, Int. Commun. Heat Mass Transfer 24 (5) (1997) 709–724.
[19] R.C. Progelhof, J.L. Throne, R.R. Ruetsch, Methods for predicting the thermal conductivity of composite systems: a review, Polym. Eng. Sci. 16 (9) (1976) 615–625.
[20] W.E. Morton, W.S. Hearle, Physical Properties of Textile Fibres, fourth ed., Woodhead Publishing Limited, 2008. pp. 179, 187, 188.
[21] P. Gibson, Multiphase Heat and Mass Transfer Through Hygroscopic Porous Media with Applications to Clothing Materials, Massachusetts (1996). pp. 36, 106, 141.
[22] B.E. Poling, J.M. Prausnitz, J.P. O'Connel, The Properties of Gases and Liquids, fifth ed., McGraw Hill, 2001. pp. 11.10, 11.13. 11.19.
[23] ISO 9073-2: Textiles – test methods for nonwovens – part 2: determination of thickness, 1995.
[24] ISO 11092:1993(E) – Textiles – physiological effects – measurement of thermal and water–vapour resistance under steady-state conditions (sweating guarded-hotplate test), 1993.
[25] Y.A. Çengel, Heat and Mass Transfer – A Practical Approach, third ed., 2007, pp. 374, 385, 468, 478, 759.
[26] Y. Li, Z.X. Luo, Physical mechanisms of moisture diffusion into hygroscopic fabrics during humidity transients, J. Text. Inst. 91 (2) (2000) 302–316.
[27] K. Prasad, W. Twilley, J.R. Lawson, Thermal Performance of Fire Fighters Protective Clothing. 1- Numerical Study of Transient Heat and Water Vapor Transfer, 2002, pp. 1–32.
[28] C. Zhang, X. Wang, Y. Lv, J. Ma, J. Huang, A new method for evaluating heat and water vapor transfer properties of porous polymeric materials, Polym. Test. 29 (5) (2010) 553–557.
[29] M.W. Haynes, D.R. Lide, Handbook of Chemistry and Physics. Available online at: <http://www.hbcpnetbase.com/>, 2012. (accessed: 09.09.2012).